ОБЪЕДИНЕННЫЙ
ИНСТИТУТ
ЯДЕРНЫХ
ИССЛЕДОВАНИЙ

Дубна

00-202

E4-2000-202

V.A.Kuz'min[1], T.V.Tetereva[2], K.Junker[3],
A.A.Ovchinnikova[2]

THE TOTAL ORDINARY MUON CAPTURE RATES. MICROSCOPIC CALCULATIONS FOR HEAVY NUCLEI

Submitted to «Nuclear Physics A»

[1]E-mail: kuzmin@thsun1.jinr.ru
[2]Skobeltsyn Nuclear Physics Institute, Lomonosov Moscow State University, Moscow, Russia
[3]Paul Scherrer Institute, CH-5232 Villigen-PSI, Switzerland

2000

1 Introduction

Investigations of the muon capture by atomic nuclei are mainly aimed at determining the constants of weak nucleon current in nuclear medium. The general interest is concentrated on the weak axial-vector g_A and pseudoscalar g_P couplings. The observables of nuclear muon capture are calculated as functions of g_A and g_P and are compared to corresponding experimental data. The Radiative Muon Capture (RMC) is traditionally considered as the most promising source of the information about g_P [1]. The sensitivity to g_P could be increased if one considers the ratio of the total RMC rate to the total Ordinary Muon Capture (OMC) rate [2, 3]. Therefore, the problem arises, how to make consistent calculations of the total RMC and OMC rates within the same nuclear model.

Also, the investigation of total OMC rates is of interest itself because it opens the way of determining g_A independently of the beta-decay. In contrast to the beta-decay all the final nucleus states with a noticeable transition strength can be populated in the muon capture. Therefore, small variations in low-energy parts of theoretical strength functions give no dramatic changes in the calculated OMC rates, as it happens in the calculations of $\log(ft)$ values. An additional advantage of the muon capture compared to the beta decay is that the total OMC rates are measured for many stable and long-lived nuclei. Therefore, one can by OMC study not only how g_A varies with the nuclear mass but more delicate effects, as the isotopic dependence of effective constants of weak interactions between the leptons and nucleons.

General situation with studying the total Ordinary Muon Capture (OMC) rates on nuclei could be described as follows. The total OMC rates were measured for many nuclei with rather a high precision. The measurements have been made for a long time, and for many nuclei the experimental data are available now [4]. But the uncontroversial interpretation of experimental information is not achieved yet. The main reason is that the theoretical description of the OMC and RMC requires to take account of the nuclear response correctly.

The theoretical investigation of nuclear muon capture has rather a long story. Up to now, three different approaches have been developed for the calculations of total (exclusive) OMC rates on complex nuclei. The first approach is based on the closure approximation and on the related method of sum rules. In both the cases, the energy of an outgoing neutrino is replaced by some average value which is a parameter of the theory in fact. Afterwards, the OMC rate is obtained by the closure relation for the states of final nucleus [5, 6]. The second approach utilizes the local density approximation. In this approach, the OMC rate is calculated for infinite an uniform nuclear matter as a function of the proton and neutron densities. The OMC rate

for a finite-size nucleus is then calculated either by integrating this function over the realistic density distribution or by determining its value for a certain value of the nuclear matter density [7, 8]. The common drawback of both approaches is that the nuclear muon capture is considered without any connections to other processes which take place in a nucleus. Also, the collective nature of nuclear response to external fields is lost. Therefore, we prefer the third approach. The (exclusive) OMC rates are calculated for each state of a product nucleus, and the total rate is obtained as a sum of these rates

$$\Lambda_{\rm tot} = \sum_f \Lambda_{fi}. \qquad (1)$$

The calculations of Refs. [9, 10, 11, 3, 12] are carried out within this approach.

In the present paper, we study the total OMC rates on heavy nuclei within the microscopic approach to the description of the nuclear structure. The one-body effective Hamiltonian of nuclear OMC is obtained within the Morita and Fujii formalism [13]. The wave function of a bound muon and the muon binding energy are calculated by approximate formulae [14] that take account of the finite size of nucleus. The nuclear matrix elements of the effective OMC Hamiltonian and the excitation energies of states of a product nucleus are calculated within the Quaiparticle Random Phase Approximation (QRPA), an extension of the usual RPA to the nonclosed shell nuclei. For first the time the velocity-dependent terms are included into calculations with nucleon single-particle states having the correct asymptotic behaviour, because the nucleon single-particle wave functions are calculated for the Saxon-Woods potential.

2 Effective Hamiltonian of Nuclear Muon Capture

The total rate of OMC is calculated by summing the rates Λ_{fi} for partial transitions $i \to f$. In a spherically symmetric nucleus Λ_{fi} is equal [15] to

$$\begin{aligned}\Lambda_{fi} = \; & [G\cos\Theta_C]^2\,(E_\nu)^2(1-\tfrac{E_\nu}{M_i+m_\mu})\,\tfrac{2J_f+1}{2J_i+1} \\ & \textstyle\sum_u (M_u^2(u)+M_u^2(u+1)+M_u^2(-u)+M_u^2(-u-1)),\end{aligned}$$

where nuclear amplitudes $M_u(\kappa)$ are amplitudes of the transition, at which the neutrino is created in the state with energy E_ν and angular quantum number κ ($\kappa = l$ for $j = l-1/2$ and $\kappa = -l-1$ for $j = l+1/2$); u is the angular momentum transferred to the nucleus. These amplitudes are combinations of the weak form factors with

nuclear matrix elements

$$
\begin{aligned}
M_u(u) = \quad & \sqrt{\frac{2}{2u+1}}\Big(\sqrt{u}C_V[0uu] - \sqrt{\frac{u+1}{3}}G_A[1uu] \\
& -\sqrt{\frac{2u+1}{3}}\frac{g_V}{M}[1u-1up]\Big), \\
M_u(-u-1) = \quad & \sqrt{\frac{2}{2u+1}}\Big(\sqrt{u+1}C_V[0uu] + \sqrt{\frac{u}{3}}G_A[1uu] \\
& -\sqrt{\frac{2u+1}{3}}\frac{g_V}{M}[1u+1up]\Big), \\
M_u(-u) = \quad & \sqrt{\frac{2}{2u+1}}\Big(-\sqrt{\frac{2u+1}{3}}(G_A - \frac{u}{2u+1}G_P)[1u-1u] \\
& +\sqrt{\frac{u(u+1)}{3(2u+1)}}G_P[1u+1u] - \sqrt{u}\frac{g_A}{M}[0uup] \\
& +\sqrt{\frac{u+1}{3}}\frac{g_V}{M}[1uup]\Big), \\
M_u(u+1) = \quad & \sqrt{\frac{2}{2u+1}}\Big(-\sqrt{\frac{u(u+1)}{3(2u+1)}}G_P[1u-1u] + \sqrt{\frac{2u+1}{3}}(G_A \\
& -\frac{u+1}{2u+1}G_P)[1u+1u] + \sqrt{u+1}\frac{g_A}{M}[0uup] + \sqrt{\frac{u}{3}}\frac{g_V}{M}[1uup]\Big)
\end{aligned}
\tag{2}
$$

The "large" form factors are defined by

$$
\begin{aligned}
G_V = \quad & g_V(q^2)(1 + E_\nu/2M) + g_S(q^2) \\
G_A = \quad & g_A(q^2) - (g_V(q^2) + g_M(q^2))(E_\nu/2M) \\
G_P = \quad & (g_P(q^2) - g_A(q^2) - g_T(q^2) - g_V(q^2) - g_M(q^2))(E_\nu/2M).
\end{aligned}
$$

The nuclear matrix elements are defined

$$
\begin{aligned}
[0uu] = \quad & \langle J_f \parallel \sqrt{\frac{1}{4\pi}}\sum_{k=1}^{A}\phi_\mu(r_k)\,\tau_k^+\,j_u(E_\nu r_k)\,Y_u(\hat{r}_k) \parallel J_i\rangle/\sqrt{2J_f+1} \\
[1wu] = \quad & \langle J_f \parallel \sqrt{\frac{3}{4\pi}}\sum_{k=1}^{A}\phi_\mu(r_k)\,\tau_k^+\,j_w(E_\nu r_k)\,[\sigma \otimes Y_w(\hat{r}_k)]_u \parallel J_i\rangle/\sqrt{2J_f+1} \\
[1wup] = \quad & i\langle J_f \parallel \sqrt{\frac{3}{4\pi}}\sum_{k=1}^{A}\phi_\mu(r_k)\,\tau_k^+\,j_w(E_\nu r_k)\,[Y_w(\hat{r}_k) \otimes p_k]_u \parallel J_i\rangle/\sqrt{2J_f+1} \\
[0uup] = \quad & i\langle J_f \parallel \sqrt{\frac{1}{4\pi}}\sum_{k=1}^{A}\phi_\mu(r_k)\,\tau_k^+\,j_u(E_\nu r_k)\,Y_u(\hat{r}_k)\,(\vec{p}_k,\vec{\sigma}_k) \parallel J_i\rangle/\sqrt{2J_f+1}.
\end{aligned}
\tag{3}
$$

The spherical Bessel function is defined by $j_u(x) = \sqrt{\pi/2x}J_{u+1/2}(x)$. The tensor product of two spherical tensor operators is

$$
[\sigma \otimes Y_w(\hat{r})]_{u,m_u} = \sum_{m,m_w}\langle 1m\,wm_w|um_u\rangle\,\sigma_m Y_{w,m_w}(\hat{r}).
$$

The radial wave function of the bound muon is $\phi_\mu(r)$. The isospin operator τ^+ is defined here by $\tau^+|p\rangle = |n\rangle$.

From these formulae one can see that the capture rate depends strongly on the energy of an outgoing neutrino

$$E_\nu = (m_\mu - |\epsilon_{1S}| + M_i - M_f - E^*)(1 - \frac{m_\mu - |\epsilon_{1S}| + M_i - M_f - E^*}{2(m_\mu + M_i)}),$$

For a large Z nucleus, the muon binding energy ϵ_{1S} must be calculated for the finite size nuclear charge distribution. The excitation energy of the final nuclear state E^* influences the capture rate mainly through the neutrino energy. To calculate the rates of nuclear OMC, one should know the energy of the considered transition (in order to determine E_ν) and matrix elements of one-body operators (3). The matrix elements of the effective Hamiltonian of nuclear OMC and the energies of excited states measured from the ground state are calculated in the present paper within QRPA. Indeed, QRPA is the prescription how one can obtain the excitation energies and matrix elements of one-body transition operators taking into account the interaction between particle hole excitations. The constants of nuclear residual interactions are fixed by analyzing the strength functions of charge-exchange spin-flip excitations. The structure of these excitations is similar to the structure of the excitations created in the nuclear muon capture. A large amount of the experimental data on spin-flip excitations has been collected up to now.

3 Nuclear Structure Calculations

The energies of excited states of the product nucleus and the matrix elements between the wave functions of the ground and excited states are calculated in the framework of QRPA. The Hamiltonian of the nuclear model consists of the mean field potentials, the monopole pairing interaction between the like particles and the residual interactions

$$H_M = \sum_{t_3=\pm 1/2} \Big(H_{\rm mean}(t_3) + H_{\rm pair}(t_3) \Big) + H_{\rm resid},$$

here the third projection of isospin t_3 is equal to $1/2$ for neutrons and $(-1/2)$ for protons. Mean field and pairing Hamiltonians are presented in the second-quantized form

$$\begin{aligned} H_0(t_3) = \; & H_{\rm mean}(t_3) + H_{\rm pair}(t_3) = \sum_{j,m} E_{jt_3} a^\dagger_{jmt_3} a_{jmt_3} \\ & - \frac{G_{t_3}}{4} \sum_{jm,j'm'} (-1)^{j-m+j'-m'} a^\dagger_{jmt_3} a^\dagger_{j,-mt_3} a_{j',-m't_3} a_{j'm't_3} \end{aligned} \tag{4}$$

The Saxon-Woods potential with spin-orbital interaction is used as the mean field potential. Its parameters and the constants of the monopole pairing interaction $G_{n,p}$

are chosen separately for neutrons and protons [16]. We use the effective isospin-invariant separable residual interaction

$$\begin{aligned} H_{\rm resid} = & -\frac{1}{2}\sum_{L,M}(\kappa_0^L + \kappa_1^L(\vec{\tau}_1\cdot\vec{\tau}_2))Q^\dagger_{LM}(1)Q_{LM}(2) \\ & -\frac{1}{2}\sum_{L,J,M}(\kappa_0^{LJ} + \kappa_1^{LJ}(\vec{\tau}_1\cdot\vec{\tau}_2))Q^\dagger_{LJM}(1)Q_{LJM}(2)\ , \end{aligned} \tag{5}$$

that is a sum of the products of multipole (Q_{LM}) and spin-multipole (Q_{LJM}) single-particle operators. It's convenient to decompose the scalar product of isospin Pauli matrices as

$$(\vec{\tau}_1\cdot\vec{\tau}_2) = 4t_1^0t_2^0 + 2t_1^-t_2^+$$

Afterwards,

$$Q_{LM} = \sum_{j'm't'_3,jmt_3}\langle j'm't'_3|i^L f_L(r)\,Y_{LM}\,\tau^k|jmt_3\rangle a^\dagger_{j'm't'_3}a_{jmt_3}$$

and

$$Q_{LJM} = \sum_{j'm't'_3,jmt_3}\langle j'm't'_3|i^L f_{LJ}(r)\,[Y_L\otimes\sigma]_{JM}\,\tau^k|jmt_3\rangle a^\dagger_{j'm't'_3}a_{jmt_3}\ ,$$

where τ^k is the isospin operator from the set $\hat{1}$, t^0, t^+, and t^-; $f_L(r)$ and $f_{LJ}(r)$ are the radial form factors of residual interaction operators. There are two popular radial form factors $f_{LJ}(r)$ of single-particle operators [17]. The first form factor is

$$f_L(r) = f(r)_{LJ} = r^L. \tag{6}$$

and the second one is

$$f_L(r) = f(r)_{LJ} = f(r) = \frac{d}{dr}U(r), \tag{7}$$

where $U(r)$ is the central part of shell potential.

The interaction that contains the product $t_1^-t_2^+$ led to the particle-hole excitations changing the charge of the nucleus. Therefore, this charge-exchange interaction can be used for describing the β-decay, μ-capture, (p,n)- and (n,p)-reactions. The corresponding single-particle operators are

$$\Omega_{JM} = \sum_{j_nm_n,j_pm_p}\langle j_nm_n|O_{JM}t^+|j_pm_p\rangle\, a^\dagger_{j_n,m_n}a_{j_p,m_p}$$

and Hermitian conjugated to them. Here O_{JM} is either multipole $i^Jf_J(r)Y_{JM}(\hat{r})$ or spin-multipole $i^Lf_{LJ}(r)[Y_L(\hat{r})\otimes\sigma]_{JM}$ operator.

Hamiltonian (5) contains scalar products $([Y_{L-1}(\hat{r}_1)\otimes\sigma_1]_L, [Y_{L-1}(\hat{r}_2)\otimes\sigma_2]_L)$ and $([Y_{L+1}(\hat{r}_1)\otimes\sigma_1]_L, [Y_{L+1}(\hat{r}_2)\otimes\sigma_2]_L)$. The tensor interaction that mixes

$[Y_{L-1}(\hat{r}_1)\otimes\sigma_1]_{LM}$ and $[Y_{L+1}(\hat{r}_2)\otimes\sigma_2]_{LM}$ is not included in (5), because it slightly influences the properties of charge-exchange resonances at reasonable values of the coupling constant.

The Bogoliubov transformation for taking into account the pairing correlations of superconducting type is as follows:

$$a_{jmt_3} = u_{jt_3}\alpha_{jmt_3} + (-1)^{j-m}v_{jt_3}\alpha^{\dagger}_{j,-mt_3}.$$

The variational procedure

$$\delta\langle 0|H_0(t_3) - \lambda_{t_3}N_{t_3} - \sum_j \rho_j(u^2_{jt_3} + v^2_{jt_3} - 1)|0\rangle = 0$$

gives the u,v-coefficients and allows us to transit to the Independent Quasiparticles Hamiltonian:

$$H_0(t_3) \to \sum_{jm}\epsilon_{jt_3}\alpha^{\dagger}_{jmt_3}\alpha_{jmt_3}$$

where

$$\epsilon_{jt_3} = \sqrt{(E_{jt_3} - \lambda_{t_3})^2 + C^2_{t_3}} \quad \text{and} \quad C_{t_3} = \frac{G_{t_3}}{2}\sum_{j,m} u_{jt_3}v_{jt_3}\,.$$

Averaging was done over the quasiparticle vacuum state: $\alpha_{jmt_3}|0\rangle = 0$.

The residual interaction Hamiltonian is approximately diagonalized by QRPA. For that purpose, the operator of phonon destruction is introduced

$$\Omega^i_{JM} = \sum_{j_p,j_n}\left(\psi^i_{j_p,j_n}[\alpha_{j_p}\otimes\alpha_{j_n}]_{J,M} - (-1)^{J-M}\phi^i_{j_p,j_n}[\alpha_{j_p}\otimes\alpha_{j_n}]^{\dagger}_{J,-M}\right).$$

The normalization and orthogonality conditions for phonon amplitudes $\phi^i_{j_n,j_p}$ and $psi^i_{j_n,j_p}$ are

$$\Phi(i,i') = \sum_{j_p,j_n}\{\psi^i_{j_p,j_n}\psi^{i'}_{j_p,j_n} - \phi^i_{j_p,j_n}\phi^{i'}_{j_p,j_n}\} - \delta_{i,i'} = 0\,.$$

The phonon amplitudes and the excitation energies of one-phonon states are determined by the variational principle

$$\delta\Big\{\langle|\Omega^i_{JM}H_M\,{\Omega^i_{JM}}^{\dagger}|\rangle - \langle|H_M|\rangle - \omega_i\,\Phi(i,i)\Big\} = 0,$$

where $|\rangle$ is the phonon vacuum state: $\Omega^i_{JM}|\rangle = 0$. The variational principle gives the homogeneous system of linear equations

$$\begin{aligned} R^{+}_{q,q'}g^i_{q'} - \omega_i w^i_q &= 0,\\ -\omega_i g^i_q + R^{-}_{q,q'}w^i_{q'} &= 0, \end{aligned}$$

where

$$g^i_q = \psi^i_{j_p,j_n} + \phi^i_{j_p,j_n}, \qquad w^i_q = \psi^i_{j_p,j_n} - \phi^i_{j_p,j_n},$$

$$R^{\pm}_{q,q'} = \epsilon_q \delta_{q,q'} - \frac{2\kappa^{J(LJ)}}{2J+1} h_q h_{q'} u^{\pm}_q u^{\pm}_{q'} ,$$

$$\epsilon_q = \epsilon_{j_p} + \epsilon_{j_n}, \qquad u^{\pm}_q = u_{j_p} v_{j_n} \pm v_{j_p} u_{j_n} \quad \text{and} \quad h_q = \langle j_p \| O_J t^- \| j_n \rangle .$$

The amplitudes of the transitions from the even-even ground state to the excited states with total spin J, third projection of total spin M and with energies ω_i are equal to either

$$b^+_{JM}(i) = \frac{1}{\sqrt{2J+1}} \sum_{j_p, j_n} \langle j_p \| O_J t^- \| j_n \rangle (v_{j_p} u_{j_n} \psi^i_{j_p, j_n} + u_{j_p} v_{j_n} \phi^i_{j_p, j_n})$$

if the charge of the nucleus is decreased by one as in the (n,p) reaction, for example, or to

$$b^-_{JM}(i) = \frac{1}{\sqrt{2J+1}} \sum_{j_p, j_n} \langle j_p \| O_J t^- \| j_n \rangle (u_{j_p} v_{j_n} \psi^i_{j_p, j_n} + v_{j_p} u_{j_n} \phi^i_{j_p, j_n})$$

if the charge is increased during transition, as in the (p,n) reaction.

Only the effective constants of isovector residual integration κ^L_1 or κ^{LJ}_1 were varied in our calculations.

4 Parameters of nuclear model

The model describes the excited states of a product nucleus as superpositions of particle-hole (two-quasiparticle) excitations over the particle-hole (quasiparticle) vacuum state. All the information about nuclear structure is concentrated in parameters of the nuclear model Hamiltonian. There are three groups of parameters.

The first group contains the parameters of a single-particle potential that represents the mean field potential and keeps nucleons together. The Saxon-Woods potentials are used. The parameters are determined in order to reproduce the excitations energies of single-particle states of neighboring odd-mass nuclei. The potentials for protons and neutrons are selected separately.

The second set of parameters are the parameters of monopole pairing interactions. In the nuclei having non-closed shells, this interaction forms the superconducting pair correlations. We use the approximation of constant pairing interaction. Its constant is determined from the even-odd effect in the nuclear binding energies. The pairing constants are connected to the parameters of mean field in the sense that the theoretical binding energies are dependent on the single-particle energies. One set of parameters of single-particle potentials and monopole pairing is usually used in the calculations of several neighboring nuclei. These sets of parameters were determined quite long ago and were published in Ref. [16].

The last set of parameters are the parameters of a nuclear residual interaction between particle-hole excitations. This interaction causes the nuclear collective movements of small amplitude (vibrations). The residual interaction Hamiltonian is taken in a separable form. A detailed discussion of this residual interaction is given by authors of [17]. Here we would like to stress that the effective constants of residual interactions are determined by calculating the excitation energies and transition strength of collective isovector states and by a subsequent comparison with experimental data. Only isovector interactions are important for the purposes of the present paper because the charge of a nucleus is changed during the considered processes.

To reveal the sensitivity of calculated $\Lambda_{\rm tot}$ to the selection of residual interactions and to the values of their effective constants, we present the results of calculations employing both the variants of separable residual interactions (6) and (7) for several values of isovector coupling constants κ_1^{LJ}.

5 Results of calculations

In this section, we present the results of calculations of total OMC rates for spherical nuclei from different regions of the nuclear mass.

5.1 ^{90}Zr and ^{92}Mo

The distributions of transition strength of the operator σt^- (Gamow-Teller transitions) over the excitation energies have been studied in detail by reactions ^{90}Zr$(p,n)^{90}$Nb [19, 20] and ^{90}Zr$(^6$Li$,^6$He$)^{90}$Nb [21]. The strength function has a prominent peak at the energy 15.6 MeV. The transition strength in the peak region is approximately equal to 10. The total transition strength observed below 20 MeV of excitation is around 20. The total GT strength must be larger than $3(N-Z) = 30$, the value given by the Ikeda sum rule [22].

Table 1 shows how the calculated properties of GT strength function depend on κ_1^{01} and κ_1^{21}. The model of non-interacting quasiparticles (residual interaction is switched off by $\kappa_1^{01} = \kappa_1^{21} = 0$) could not give the correct position of the peak of strength function. For $L = 0$ and $J = 1$, the residual interaction (6) reduces to the simple $(\vec{\sigma},\vec{\sigma})$ interaction considered in [18]. The calculations with $\kappa_1^{01} = -23/A$ recommended in [18] correctly reproduce the position of the maximum of strength function. The results of calculations with slightly different constants $\kappa_1^{01} = -25/A$ and $\kappa_1^{01} = -28/A$) presented in Table 1 show that the position of the maximum of strength function is sensitive to κ_1^{01}. The strength in the peak region does not depend on κ_1^{01} and considerably exceeds the experimentally observed one. So, the best value of the effective constant for residual interaction (6) is $\kappa_1^{01} = -23/A$.

Table 1: Properties of charge-exchange 1^+ excitations in ^{90}Zr calculated with two variants of residual interactions.

$\kappa_1^{01}A$	σt^- as in (p,n) reaction				σt^+ as in (n,p) reaction			
	Energy of maximum	$B^-(GT)$			Energy of maximum	$B^+(GT)$		
		total	in max.	below max.		total	in max.	below max.
0.00	11.84	32.06	16.96	13.79	5.34	3.32	2.21	0.00
$f(r) = dU/dr$								
-0.23	14.93	31.89	20.88	6.23	5.62	3.15	1.31	0.00
-0.33	15.76	32.03	19.88	4.67	5.68	3.30	1.14	0.00
-0.43	16.36	32.21	18.41	3.74	5.73	3.47	1.03	0.00
$f_L(r) = r^L$								
-23.0	15.73	30.63	23.83	5.32	5.63	1.89	1.12	0.00
-25.0	16.09	30.56	23.98	4.86	5.65	1.82	1.07	0.00
-28.0	16.63	30.05	23.86	4.28	5.67	1.72	0.99	0.00

Table 1 shows that the calculated energy of the GT resonance is less sensitive to κ_1^{01} for residual interaction with form factor (7). The correct position of the resonance is reproduced at $\kappa_1^{01} = -0.33/A$. Simultaneously, the strength in the resonance region and below it is considerably less than of the corresponding strength calculated with interactions (6) (24.6 to be compared with 29.2) and is closer to the experimental value. The rest of the transition strength locates at high-excited 1^+ states [23]. Recently, the new experimental data about the GT transition strength at the highest excitation energies were published [20]. The total $B(GT)$ calculated with residual interaction (7) is equal to 32.0. This value agrees with the experimental value 34.2 ± 1.6 obtained in [20] by multipole decomposition of experimental cross sections of $^{90}\mathrm{Zr}(p,n)^{90}\mathrm{Nb}$ reaction.

From this consideration one can conclude that the residual interaction (7) provides a better description of the σt^- strength function than the interaction (6).

The results of recent measurements of the σt^+ transition strength in $^{90}\mathrm{Zr}(n,p)^{90}\mathrm{Y}$ [24] could also be compared with the results of calculations. In this reaction, the charge of the nucleus decreases as in muon capture. The σt^+ strength summed over experimentally observed states is $B_\Sigma^+(GT) = 1.0 \pm 0.3$ [24]. The calculation with interaction (6) gives the following distribution of the transition strength. The considerable part of transition strength is concentrated at the first 1^+ state of $^{90}\mathrm{Y}$. The other 1^+ states have excitation energies between 10 and 15 MeV. For each of these states, $B^+(GT) < 0.2$.

The σt^+ strength function calculated with $f(r) = dU/dr$ interaction (7) differs from the strength function obtained with interaction (6). The $B_\Sigma^+(GT)$ calculated with interaction (7) is almost three times of $B_\Sigma^+(GT)$ for interaction (6). This is due to highly excited states absent in the calculations with $f(r) = r^L$ interaction. As before, the strongest transition goes to the first 1^+ of $^{90}\mathrm{Y}$, but the strengths of transitions, going to 1^+ states with energies between 5 and 15 MeV, are comparable to $B_1^+(GT)$. So, the transition strength is distributed over the excitation energies more uniformly, and the shape of the theoretical strength function is closer to the experimental one.

It should be noted that the energy of the first 1^+ state calculated for each of two residual interactions does not depend on κ_1^{01}, and the corresponding $B_1^+(GT)$ decreases slightly when $|\kappa_1^{01}|$ grows. It shows that already in $^{90}\mathrm{Zr}$ the neutron excess prevents the creation of low-lying collective 1^+ states in $^{90}\mathrm{Y}$. The residual interaction with $f(r) = dU/dr$ couples single-particle states with wave functions having the same orbital quantum numbers and different number of nodes in the radial parts. Due to residual interaction (7), these particle-hole excitations interact with particle-hole states consisting of the members of the one spin-orbital multiplet and create

collective high-excited states [23]. The transitions to those states increase $B^+_\Sigma(GT)$.

It was shown in [3] that the calculated values of OMC rates are rather unsensitive to the constants of multipole residual interactions κ^J_1. Nevertheless, the constant of isovector monopole residual interaction κ^0_1 can be determined by the description of isobar analog state (IAS). The calculated properties of 0^+ charge-exchange excitations over ^{90}Zr are presented in Table 2. The independent quasiparticle model describes 0^+ charge-exchange states as a set of non-interacting two-quasiparticles states. The states that carry the main transition strength are $(0g_{9/2})_p(0g_{9/2})_n$ and $(1d_{1/2})_p(1d_{1/2})_n$ for t^- or (p,n) branch and $(0f_{7/2})_p(0f_{7/2})_n$ and $(0d_{5/2})_p(1d_{5/2})_n$ for t^+ or (n,p) transitions. The residual interaction of both types creates a collective state in the (p,n) excitation branch and for $\kappa^0_1 = -0.43/A$ (for $f(r) = dU/dr$ residual interaction) and $\kappa^0_1 = -35.0/A$ (for $f(r) = r^L$ residual interaction) its energy coincides with the experimental energy of IAS equal to 12.0 MeV [25]. In the both cases, this state consumes almost all the t^- transition strength. In the (n,p) branch, the isovector monopole interaction with $f(r) = r^{L=0} = 1$ with constant $\kappa^0_1 = -35.0/A$ could not form the collective state and the strength function is determined by $(0f_{7/2})_p(0f_{7/2})_n$ and $(0d_{5/2})_p(1d_{5/2})_n$ two-quasiparticles state. The interaction with $f(r) = \frac{dU}{dr}$ with $\kappa^0_1 = -0.43$ is strong enough to create the collective state, approximately at the same energies where the above mentioned two-quasiparticle states are. The difference between total t^- and t^+ transition strengths is constant and does not depend on the residual interaction.

Therefore, it is possible to use strength functions for determining the constants of isovector residual interactions κ^{01}_1 and κ^0_1. For the constants of residual interactions (6) for $L > 0$, we use the relations

$$\kappa^{LJ}_1 = \frac{\kappa^{01}_1}{\langle r^{2L} \rangle} \tag{8}$$

and the constants of residual interaction (7)

$$\kappa^{LJ}_1 = \kappa^{01}_1. \tag{9}$$

In the calculations of total OMC rates, the final states with total angular momenta and parities equal to $J^\pi = 0^\pm$, $1^\pm$, $2^\pm$ and $3^\pm$ were taken into account. The contribution of the final states with $J > 3$ is found to be less than 1%.

The calculated OMC rates for ^{90}Zr are presented in Table 3 and in Fig. 1. The residual interactions of both types were used in the calculations. The OMC rates shown in the Tables and in the Figures are calculated for $g_P/g_A = 6.0$. The capture rates are shown in the figures by the running sums

$$\Lambda(E) = \sum_{k:\, E_k < E} \Lambda_k. \tag{10}$$

Table 2: Properties of charge-exchange 0^+ excitations in ^{90}Zr calculated with two variants of residual interactions.

$\kappa_1^0 A$	t^-				t^+			
	Energy of maximum	B^-			Energy of maximum	B^+		
		total	in max.	below max.		total	in max.	below max.
0.00	4.62	10.14	8.62	0.00	16.17	0.29	0.07	0.13
				$f(r) = dU/dr$				
-0.33	10.99	10.58	8.30	0.37	18.08	0.72	0.55	0.16
-0.43	12.00	10.70	7.94	0.14	18.34	0.84	0.67	0.16
-0.53	12.81	10.81	7.44	0.07	18.56	0.96	0.79	0.15
				$f_L(r) = r^L$				
-23.00	10.35	10.04	7.87	1.78	16.91	0.18	0.05	0.07
					16.20		0.04	
-25.00	10.71	10.03	8.29	1.32	16.92	0.18	0.05	0.07
					16.20		0.04	
-28.00	11.28	10.02	8.68	0.88	16.92	0.17	0.05	0.07
					16.20		0.04	
-31.00	11.87	10.02	8.88	0.62	16.92	0.16	0.05	0.06
					16.20		0.04	
-34.00	12.46	10.01	8.96	0.45	16.93	0.15	0.05	0.06
					16.20		0.04	
-37.00	13.06	10.00	8.97	0.34	16.93	0.15	0.04	0.05
					16.21		0.03	

Table 3: The rates of OMC (in $10^5\,s^{-1}$) on ^{90}Zr summed over the final states with specific spin and parity J^π

$\kappa_1^{LJ}A$	final states, J^π								total
	0^+	0^-	1^+	1^-	2^+	2^-	3^+	3^-	rate
0.00	4.9	3.6	24.3	43.4	15.2	19.3	11.6	3.3	125.6
	3.9	2.8	19.3	34.6	12.1	15.4	9.2	2.6	100.0%
$f(r) = dU/dr$									
-0.23	5.3	2.2	28.3	27.3	8.5	12.3	5.5	1.4	90.8
	5.9	2.5	31.2	30.0	9.3	13.5	6.0	1.6	100.0%
-0.33	5.3	2.2	29.1	25.1	7.4	11.2	4.4	1.2	85.8
	6.2	2.5	33.9	29.2	8.6	13.1	5.2	1.4	100.0%
-0.43	5.3	2.2	29.9	23.5	6.6	10.5	3.7	1.0	82.8
	6.4	2.6	36.1	28.4	8.0	12.7	4.5	1.2	100.0%
$f_L(r) = r^L$									
-23.0	4.7	1.9	23.4	27.2	10.2	12.2	7.1	1.9	88.7
	5.3	2.2	26.4	30.6	11.5	13.8	8.0	2.2	100.0%
-25.0	4.7	1.9	23.2	27.2	10.0	11.8	6.9	1.9	86.9
	5.5	2.2	26.7	26.5	11.5	13.6	7.9	2.2	100.0%
-28.0	4.7	1.8	23.0	25.7	9.6	11.3	6.5	1.8	84.4
	5.6	2.1	27.2	30.4	11.4	13.4	7.8	2.1	100.0%

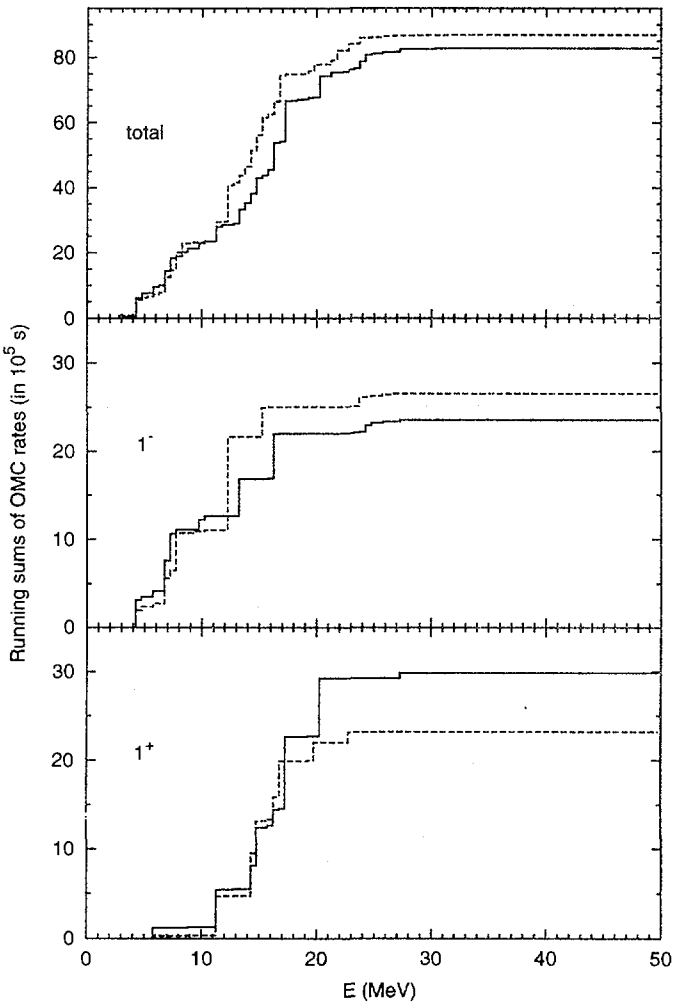

Figure 1: Runnins sums of OMC for ^{90}Zr: total and for for the states with $J^\pi = 1^\pm$. Solid lines: results of calculations with residual interaction (7), dashed lines — interaction (6).

The capture rates shown in Fig. 1 were calculated using the spin-multipole constants determined from (p,n) and (n,p) reaction data, $\kappa_1^{01} = -0.33/A$ for the interaction (6) and $\kappa_1^{01} = -23.0/A$ for the interaction (7). For multipole interactions $\kappa_1^{0} = -0.43/A$ and $\kappa_1^{01} = -35.0/A$. Figure 1 shows that the main difference in the calculated values of total capture rates originates from the muon captures populating highly excited states. This difference is biggest for 1^+ final states. The total capture rates calculated with both types of residual interactions agree with each other (the difference for optimal constant sets is less than 5%). But there are large variations in the results for capture rates feeding the states with specific values J^π. In general, the total muon capture rates on nuclei with $A \sim 90$ calculated with $f(r) = r^L$ residual interaction are larger than the ones calculated with $f(r) = dU/dr$.

Because for Zr the experimental $\Lambda_{\rm tot} = 86.6 \cdot 10^5\,{\rm s}^{-1}$ [4], one can conclude that the calculations describe the experimental data well. The comparison of the experimental $\Lambda_{\rm tot}$ with the theoretical results obtained in the present paper has a semi-qualitative character, because theoretical rates are calculated for a specific isotope mainly, but the capture rates have been measured on the natural mixture of isotopes.

The theoretical $\Lambda_{\rm tot}$'s are not very sensitive to g_P/g_A: in ^{90}Zr $\Lambda_{\rm tot}$ varies from $85.5 \cdot 10^5\,{\rm s}^{-1}$ to $76.8 \cdot 10^5\,{\rm s}^{-1}$ when g_P/g_A increases from 4.0 to 12.0.

The calculations reveal that the contributions of velocity-dependent matrix elements $[1wup]$ and $[0uup]$ to $\Lambda_{\rm tot}$ are rather small. $\Lambda_{\rm tot}$ changes less than 2% when $[1wup]$ and $[0uup]$ are discarded. Therefore, the direct test does not confirm the estimations made in [11] that the velocity-dependent matrix elements provide 12–15% of the total OMC rate.

According to the calculations, the 1^+ state with an excitation energy near 5 MeV, that strongly reveals itself in $^{90}{\rm Zr}(n,p)^{90}{\rm Y}$ reaction gives a small contribution to the OMC rate. The explanation is that the radial matrix element of zero-order spherical Bessel function $j_0(E_\nu r)$ dominating in allowed $0^+ \to 1^+$ partial transitions is hindered by the centrifugal barrier for the two-quasiparticle state $(0g_{7/2})_n(0g_{9/2})_p$. This example shows that one cannot directly use the matrix elements obtained in (p,n) and (n,p) reactions for analyzing the muon capture data, the large $B(GT)$ does not always mean the large Λ_{fi}. The 1^+ states of product nuclei may have different appearance in different reactions, and their characteristics could be "combined" only by the microscopic nuclear model.

Another nucleus for which the capture rates are calculated is ^{92}Mo, see tables 4 and 5. The comparison of calculated total OMC rates with the experimental ones shows that for nuclei with $A \sim 90$, the calculations based on the microscopic nuclear model with both the types of residual interactions have correctly reproduced the experimental total capture rate.

Table 4: Properties of charge-exchange 1^+ excitations in ^{92}Mo calculated with two different nuclear residual interactions.

$\kappa_1^{01}A$	σt^- as in (p,n) reaction				σt^+ as in (n,p) reaction			
	Energy of	$B^-(GT)$			Energy of	$B^+(GT)$		
	maximum	total	in max.	below max.	maximum	total	in max.	below max.
0.00	11.85	28.79	16.94	10.70	4.44	5.96	4.75	0.00
$f(r) = dU/dr$								
-0.23	14.98	27.42	11.61	12.17	5.04	4.59	2.92	0.00
-0.33	15.61	27.28	16.94	4.83	5.19	4.45	2.57	0.00
-0.43	16.15	27.23	16.50	3.42	5.29	4.40	2.33	0.00
$f_L(r) = r^L$								
-23.0	15.54	26.36	18.36	6.86	5.07	3.53	2.56	0.00
-25.0	15.81	26.23	19.40	5.61	5.11	3.40	2.45	0.00
-28.0	16.25	26.06	20.20	4.47	5.16	2.23	2.29	0.00

Table 5: The rates of OMC (in $10^5\,s^{-1}$) on ^{92}Mo summed over the final states with specific spin and parity J^π

$\kappa_1^{LJ}A$	final state J^π								total
	0^+	0^-	1^+	1^-	2^+	2^-	3^+	3^-	rate
0.00	5.3	4.1	27.4	52.2	18.1	24.2	13.5	3.8	148.7
	3.6	2.8	18.4	35.1	12.2	16.3	9.1	2.6	100.0%
$f(r) = dU/dr$									
-0.23	5.6	2.5	30.5	33.3	10.1	15.6	6.5	1.7	105.8
	5.3	2.4	28.8	31.5	9.5	14.7	6.2	1.6	100.0%
-0.33	5.6	2.4	31.0	30.6	8.8	14.1	5.3	1.4	99.2
	5.6	2.4	31.3	30.8	8.8	14.2	5.4	1.4	100.0%
-0.43	5.6	2.4	31.5	28.7	7.8	13.2	4.5	1.2	95.0
	5.9	2.6	33.2	30.3	8.3	13.9	4.8	1.8	100.0%
$f_L(r) = r^L$									
-23.0	5.1	2.3	26.2	33.6	12.3	15.9	8.5	2.3	106.2
	4.8	2.1	24.6	31.6	11.6	15.0	8.0	2.1	100.0%
-25.0	5.1	2.2	26.0	32.9	12.0	15.5	8.2	2.2	104.1
	4.9	2.1	24.9	31.6	11.5	14.9	7.9	2.2	100.0%
-28.0	5.1	2.1	25.7	31.8	11.6	14.9	7.9	2.2	101.2
	5.1	2.1	25.4	31.5	11.5	14.7	7.8	2.1	100.0%

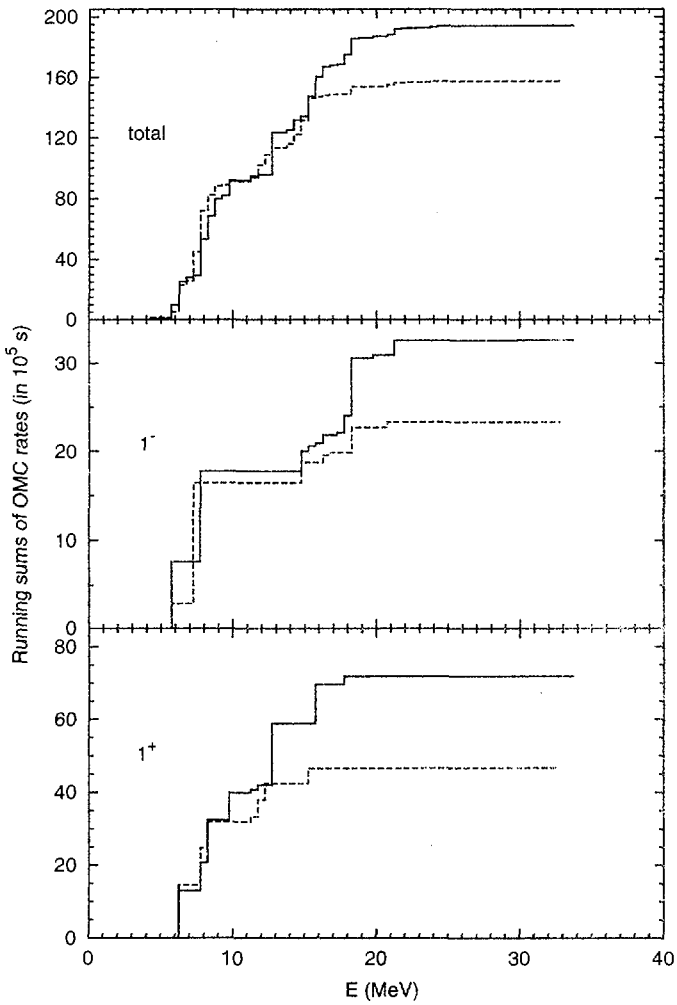

Figure 2: Runnins sums of OMC for ^{208}Pb: total and for for the states with $J^\pi = 1^\pm$. Solid lines: results of calculations with residual interaction (7), dashed lines — interaction (6).

There are differences in two calculations how the final states with specific J^π contribute to total capture rates. But, after adding all rates into the total rate, the differences almost cancel each other.

Usually, the experimental total OMC rates are known for the natural isotope mixture. So, our description of the total OMC rate on ^{92}Mo can be considered as reasonable, because ^{92}Mo is the lightest even isotope of Mo, and the capture rates decrease with growing neutron excess. The next subsection demonstrates this.

5.2 OMC on even tin isotopes

Next nuclei to be considered are the even tin isotopes $^{116-124}$Sn. These nuclei give a long chain of stable spherical isotopes. Tin isotopes have the completely occupied $0g_{9/2}$ proton subshell and subshells $0g_{7/2}$, $1d_{5/2}$, $1d_{3/2}$ and $2s_{1/2}$, which are gradually filled by neutrons. Table 6 presents the total OMC rates calculated with two sets of parameters of single-particle potentials [16]. These tables show that the calculated rates depend on the single particle potential more than on the used residual interactions.

The experimental value of the capture rate on natural tin is $106.7 \cdot 10^5\,\mathrm{s}^{-1}$ [4]. If one takes into account that the natural isotope mixture has more than 50% of ^{118,120}Sn, one can conclude that single-particle potential fitted for $A = 121, Z = 51$ gives a better description of total OMC rates.

5.3 More nucleons – more problems. ^{140}Ce and ^{208}Pb

The total OMC rates on ^{140}Ce and ^{208}Pb calculated with both the types of residual interactions are larger than experimental data, see Tables 7 and 8. The rates calculated with the nuclear residual interaction (6) are less than the ones calculated with interaction (7). The difference comes mainly from the muon capture populating the high-excited 1^+-states absent in the calculations with $f(r) = r^{l'}$ interactions. One remark related to these states should be given here. The experimental energies of collective IAS and GT (σt^-) states are described well with residual forces (6): using $\kappa_1^0 = -28.0/A$, one obtains the energy of IAS state equals to 18.94 MeV to be compared with the experimental value 18.8 MeV [25], and the calculated energy of the GT state is 19.71 MeV with $\kappa_1^{01} = -23.0/A$. Its experimental value is 19.2 MeV. More than 80% of the total calculated GT strength resides at that peak. With $f(r) = dU/dr$ residual interaction at $\kappa_1^{01} = -0.43/A$, the calculated excitation energy of the collective 1^+ state is 16.85 MeV. This state keeps approximately 50% of the total calculated GT transition strength, and more than 30% of the transition strength is shifted to the higher 1^+ states. The high-excited 1^+ states keep the

Table 6: Total OMC capture rates on Sn isotopes (in $10^5\,s^{-1}$)

Target	$\kappa_1^{01}\,A$	SW parameters		$\kappa_1^{01}\,A$	SW parameters	
nucleus	for (7)	115,49	121,51	for (6)	115,49	121,51
^{116}Sn	-0.23	139.2	130.1	-23.0	141.7	123.0
	-0.33	130.5	123.1	-25.0	138.9	120.8
	-0.43	124.9	119.0	-28.0	135.2	117.4
^{118}Sn	-0.23	130.0	122.1	-23.0	131.9	115.0
	-0.33	122.1	116.1	-25.0	129.4	112.7
	-0.43	117.1	112.4	-28.0	125.9	109.5
^{120}Sn	-0.23	121.2	111.8	-23.0	122.6	107.3
	-0.33	114.2	109.5	-25.0	120.3	104.1
	-0.43	109.8	106.3	-28.0	117.2	102.1
^{122}Sn	-0.23	113.2	107.8	-23.0	114.0	99.7
	-0.33	106.9	103.2	-25.0	118.0	97.7
	-0.43	103.0	100.6	-28.0	108.0	95.0
^{124}Sn	-0.23	105.5	101.3	-23.0	105.5	91.7
	-0.33	99.9	97.1	-25.0	103.4	89.9
	-0.43	96.5	95.1	-28.0	100.7	88.3

Table 7: The rates of OMC (in $10^5\,s^{-1}$) on ^{140}Ce summed over final states with specific spin and parity J^π

$\kappa_1^{LJ}A$	final state J^π								total
	0^+	0^-	1^+	1^-	2^+	2^-	3^+	3^-	rate
$f(r) = dU/dr$									
-0.23	11.7	3.8	55.4	39.9	20.2	21.0	10.3	3.5	165.7
	7.0	2.3	33.4	24.1	12.2	12.7	6.2	2.1	100.0%
-0.33	11.7	3.5	57.4	38.0	17.9	21.3	8.7	2.9	161.2
	7.2	2.2	35.6	23.5	11.1	13.2	5.4	1.8	100.0%
-0.43	11.7	3.4	59.2	36.7	16.2	21.7	7.7	2.5	159.0
	7.3	2.1	37.3	23.1	10.2	13.7	4.8	1.6	100.0%
$f_L(r) = r^L$									
-23.0	9.8	3.4	41.4	35.8	25.2	15.1	12.9	5.1	148.9
	6.6	2.3	27.8	24.1	16.9	10.1	8.7	3.4	100.0%
-25.0	9.8	3.3	41.2	35.1	24.7	14.8	12.5	5.0	146.3
	6.7	2.2	28.1	24.0	16.9	10.1	8.6	3.4	100.0%
-28.0	9.8	3.1	40.8	34.1	23.9	14.4	12.0	4.8	142.8
	6.9	2.2	28.5	23.9	16.7	10.1	8.4	3.4	100.0%

Table 8: The rates of OMC (in $10^5\,s^{-1}$) on ^{208}Pb summed over final states with specific spin and parity J^π

$\kappa_1^{LJ}A$	final state J^π								total
	0^+	0^-	1^+	1^-	2^+	2^-	3^+	3^-	rate
$f(r) = dU/dr$									
-0.23	15.7	3.1	70.5	33.8	29.7	29.5	10.4	5.8	198.6
	7.9	1.6	35.5	17.0	15.0	14.9	5.2	2.9	100.0%
-0.33	15.7	2.7	72.5	33.1	26.9	31.8	9.5	4.9	197.2
	8.0	1.4	36.8	16.8	13.7	16.1	4.8	2.5	100.0%
-0.43	15.7	2.4	71.9	32.6	25.0	33.2	9.9	4.3	194.2
	8.1	1.2	37.0	16.8	12.9	17.1	4.6	2.2	100.0%
$f_L(r) = r^L$									
-23.0	13.5	2.8	46.9	23.8	33.7	19.9	11.0	8.0	159.5
	8.5	1.7	29.4	14.9	21.1	12.4	6.9	5.0	100.0%
-25.0	13.5	2.6	46.7	23.3	33.0	19.8	10.7	7.8	157.4
	8.6	1.7	29.7	14.8	21.0	12.6	6.8	5.0	100.0%
-28.0	13.5	2.4	46.5	22.6	32.0	19.6	10.3	7.5	154.5
	8.7	1.6	30.1	14.7	20.7	12.7	6.7	4.9	100.0%

Table 9: The total OMC rates (in $10^5\,s^{-1}$) calculated for $g_P/g_A = 6.0$ with two different radial form factors of residual nuclear interaction.

Target	$\kappa_1^{LJ}A$ for dU/dr			$\kappa_1^{LJ}A$ for r^L			expr.
nucleus	−0.23	−0.33	−0.43	−23.0	−25.0	−28.0	[4]
^{90}Zr	90.8	85.8	82.8	88.7	86.8	84.4	86.6
^{92}Mo	105.8	99.2	95.0	106.2	104.1	101.2	92.2
^{116}Sn	130.1	123.2	119.0	123.2	120.8	117.4	
^{118}Sn	122.1	116.1	112.4	115.0	112.7	109.5	
^{120}Sn	114.8	109.5	106.3	107.3	105.1	102.1	106.7
^{122}Sn	107.8	103.2	100.6	99.7	97.7	95.0	
^{124}Sn	101.3	97.1	95.1	91.7	89.9	88.3	
^{140}Ce	165.7	161.2	159.0	148.9	146.3	142.8	114.4
^{208}Pb	198.6	197.2	194.2	159.5	157.4	154.5	134.5

Table 10: Fractional contributions of different multipoles to $\Lambda_{\rm tot}$ for ^{208}Pb (either contributions of the orbital momentum transfer or contributions of the transitions to the states with specific J^π).

Reference	ΔL							
	0		1			2		3
[9]	26		14			48		12
[10]	29		13			52		7
[11]	23		34			34		8
(a)	$\simeq 45$		$\simeq 35$			$\simeq 18$		$\simeq 2$
(b)	$\simeq 38$		$\simeq 29$			$\simeq 27$		$\simeq 5$
	J^π							
	0^+	1^+	0^-	1^-	2^-	2^+	3^+	3^-
[12]	5	36	6	14	12	28	4	2
(a)	8	37	2	17	16	14	5	3
(b)	8	30	2	15	12	21	7	5

(a) – present paper, calculations with residual interactions (7), $\kappa_1^{LJ} \cdot A = -0.43$;
(b) – present paper, calculations with residual interactions (6), $\kappa_1^{LJ} \cdot A = -25.0$.

collective state in the region below 18 MeV even if $|\kappa_1^{01}|$ is doubled.

The experimental value of Λ_{tot} for ^{208}Pb is $135 \cdot 10^5\,\mathrm{s}^{-1}$ [4]. So, both the calculations overestimate the total capture rate considerably. Therefore, it is interesting to compare our results to the ones of previous papers where a good description of the experimental data was achieved [9, 11]. There is a difficulty in comparison because the authors of [9, 10, 11] have presented the relative contributions to Λ_{tot} of different transfers of orbital momentum L. To compare these data to our results, we assume that the transitions to 0^+ and 1^+ final states go by $L = 0$, the transitions to $0^-, 1^-, 2^-$ are accompanied by the transfer of $L = 1$ orbital momentum, and so on. By this assumption, we suppose that $|[1\,J - 1\,J]| >> |[1\,J + 1\,J]|$. Test shows that deleting of $[1\,J + 1\,J]$ reduces the corresponding Λ_{fi} less than 10%. The obtained fractional contributions are collected into Table 10, that shows that the numbers obtained in this paper differ from the ones of [9, 10, 11] mainly by the contributions of the transitions $0^+ \to 1^+$. The dominating role of $0^+ \to 1^+$ transitions is revealed in recent calculations of [12], too. The total OMC rate on ^{208}Pb calculated in the present work with residual interaction (6) agrees well with the value $\Lambda_{\mathrm{tot}}(^{208}\mathrm{Pb}) = 161 \cdot 10^5\,\mathrm{s}^{-1}$ obtained in [12] with δ-function residual interactions.

6 Discussions

This paper presents the first attempt to calculate explicitly the velocity-dependent terms with single particle wave functions having the correct asymptotics. Previous works gives only estimations, see for example [11]. The gradient terms are directly calculated now, and their contribution to the $\Lambda_{\mathrm{tot}}^{\mathrm{theor}}$ is shown to be small. Certain confusion may be here. In general, the notion of "velocity-dependent" terms is used for all terms coming from small components of nucleon 4-spinors. Under derivation of the effective muon capture Hamiltonian [15], part of these terms are transformed with the law of momentum conservation

$$\vec{p} + \vec{\mu} = \vec{n} + \vec{\nu}, \quad |\vec{\mu}| \approx 0, \quad \text{and} \quad \vec{n} = \vec{p} - \vec{\nu}.$$

As a result, only the gradient acting on proton wave functions is left. We have explicitly shown that the matrix elements with proton gradient give a minor contribution to the capture rate. So, one can conclude that the main effect of velocity-dependent terms is already accounted in the effective Hamiltonian by the momentum conservation.

Common people (in nuclear physics) have general feelings that the total OMC rates could be described correctly without any problem. There are some papers showing it, for example, [11]. So, our failure in reproducing the total OMC rates on

^{140}Ce and ^{208}Pb must be explained. A similar problem with reproducing the total OMC rate for ^{208}Pb is faced by authors of recent paper [12], too.

7 Conclusions

Our calculations show the that total OMC rates are not sensitive to the constants of nuclear residual interactions. Simultaneously, theoretical total OMC rates may strongly depend on the nuclear residual interactions used in the calculations. The main distinctions in Λ_{tot} calculated with different residual interactions come from the differences in the description of GT transitions, $0^+ \rightarrow 1^+$, especially, at high excitation energies.

The theoretical Λ_{tot} being compared to the experimental rate shows that the calculations with free values of g_A and g_P describe reasonably the experimental data for the medium nuclei (^{90}Zr, $^{116-124}$Sn). Therefore, there is no need in the renormalization of g_A in these mass regions.

For heavier nuclei (^{140}Ce, ^{208}Pb), the theoretical Λ_{tot}'s exceed considerably the experimental values. Therefore, some renormalization of g_A is essential for reproducing the experimental Λ_{tot} in heavy nuclei. But this renormalization is model-dependent, because its value depends on the nuclear residual interactions, as Tables 7 and 8 show.

References

[1] I.S. Towner, J.C. Hardy, The Nucleus as a Laboratory for Studying Symmetries and Fundamental Interaction, in Eds. E.M. Henley, W.C. Haxton; Singapore, New Jersey, London, Hong Kong: World Scientific Publ. Co. Pte. Ltd., 1995, p. 183.

[2] M. Gmitro, A.A. Ovchinnikova, T.V. Tetereva, 1986, Nucl. Phys. A **453**, 685.

[3] R.A. Eramzhyan, V.A. Kuz'min, and T.V. Tetereva, 1998, Nucl. Phys. A **642**, 428.

[4] T. Suzuki, D.F. Measday, J.P. Roalsvig, 1987, Phys. Rev. C **35**, 2212.

[5] B. Goulard, H. Primakoff, 1974, Phys. Rev. C **10**, 2034.

[6] J. Navarro, J. Bernabeu, J.M. Gomez, J. Martorell, 1987, Nucl. Phys. A **375**, 361.

[7] H.C. Chiang, E. Oset, P. Fernandez de Cordoba, 1990, Nucl. Phys. A **510**, 591.

[8] H.W. Fearing, M.S. Welsh, 1992, Phys. Rev. C **46**, 2077.

[9] G.G. Bunatian, 1966, Sov. J. Nucl. Phys. **3**, 613.

[10] N. Auerbach, L. Zamick, A. Klein, 1982, Phys. Lett. B **118**, 256;
N. Auerbach, A. Klein, 1984, Nucl. Phys. A **422**, 480.

[11] M.G. Urin, and O.N. Vyazankin, 1992, Nucl. Phys. A, **537**, 534.

[12] E. Kolbe, K. Langanke, P. Vogel, 2000, Preprint arXiv:nucl-th/0006007.

[13] M. Morita, and A. Fujii, 1960, Phys. Rev. **118**, 606.

[14] G.E. Pustovalov, 1959, Sov. Phys. JETP, **36(9)**, 1288.

[15] V.V. Balashov, G.Ya. Korenman, and R.A. Eramzhyan, "Poglozhenie mezonov atomnymi yadrami", M., 1978 (in Russian).

[16] V.Yu. Ponomarev, *et al*, 1979, Nucl. Phys. A **323**, 446.

[17] A.I. Vdovin. and V.G. Soloviev, 1983, Sov. J. Part. Nucl. **14**, 237.

[18] C. Gaarde, *et al*, 1981, Nucl. Phys. A **369**, 258.

[19] D.E. Bainum, J. Rapaport, C.D. Goodman, *et al.* 1980, Phys. Rev. Lett. **44**, 1751.

[20] T. Wakasa, H. Sakai, H. Okamura, *et al.* 1997, Phys. Rev. C **55**, 2909.

[21] M. Moosburger, E. Aschenauer, H. Dennert, *et al.* 1998, Phys. Rev. C **57**, 602.

[22] K. Ikeda, S. Fujii, and J.I. Fujita, 1963, Phys. Lett. **63**, 271.

[23] V.A. Kuz'min, 1995, Phys. Atom. Nucl. **58**, 368;
K. Junker, V.A. Kuz'min, T.V. Tetereva, 1999, Eur. Phys. J. A **5**, 37.

[24] K.J. Raywood, B.M. Spicer, S. Yen, *et al.* 1990, Phys. Rev. C **41**, 2836.

[25] W.J. Courtney, and J.D. Fox, 1975, At. Data and Nucl. Data Tabl. **15**, 141.

Received by Publishing Department
on September 4, 2000.